

Heavy ion fusion science virtual national laboratory: highlights for 2007

Reported by Grant Logan, Director of the Heavy Ion Fusion Science Virtual National Laboratory (HIFS-VNL)

In FY2007, the U.S. heavy ion fusion science program has made significant experimental and theoretical progress in simultaneous transverse and longitudinal beam compression, ion-beam-driven warm dense matter targets, high brightness beam transport, advanced theory and numerical simulations, and heavy ion target designs for fusion. First experiments combining radial and longitudinal compression of intense ion beams propagating through background plasma resulted in on-axis beam densities increased by 700X at the focal plane. With further improvements planned in 2007, these results will enable initial ion beam target experiments in warm dense matter to begin next year at LBNL. We are assessing how these new techniques apply to low-cost modular fusion drivers and higher-gain direct-drive targets for inertial fusion energy.

Combined transverse and longitudinal compression of beams with neutralized plasma - Recent experiments in NDCX, (see Fig. 1) have combined neutralized drift compression with a new final focusing solenoid (FFS) and a new target chamber. The FFS was installed with a new beam target chamber, and the plasma density was measured before installing on the NDCX beam line. Two Filtered Cathodic Arc Plasma Sources (FCAPS) streamed aluminum metal plasma upstream toward the exit of the FFS, and a Langmuir probe was driven from the upstream end of the FFS toward the focal plane of the magnet, 18.27 cm downstream of the midplane

of the FFS. The target focal plane beam diagnostics were a multiple-pinhole Faraday cup, and a scintillator (the light emission of which was detected using a gated CCD camera). FWHM's of 2 mm and 3 mm were measured when the FFS field was 5T and 0 T, respectively, (See Fig. 2). The peak

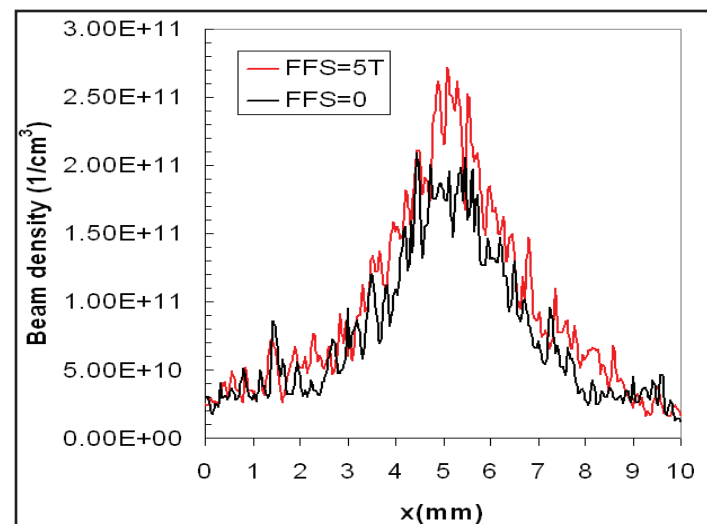


Figure 2: Beam density profiles at the target focal plane with the final focus solenoid on (FFS=5T) and off (FFS=0). The corresponding focal spot FWHM = 2 mm with FFS=5T and 3 mm with FFS=0.

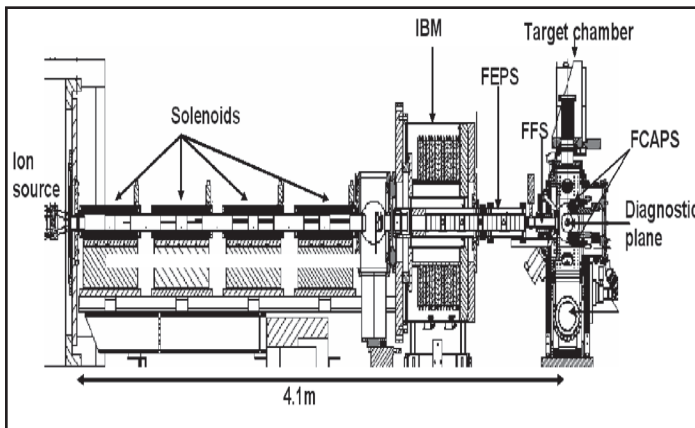


Figure 1: Elevation view of the NDCX. Left to right: 315 keV, 25 mA K⁺ ion source, solenoid transport section, induction bunching module (IBM) which imparts the velocity ramp that starts the drift compression of a 150 ns slice of the injected beam, ferroelectric plasma source (FEPS) which neutralizes the longitudinal drift compression region, 5T final focus solenoid (FFS), and new target chamber containing diagnostics at the target plane and two filtered cathodic arc plasma sources (FCAPS).

intensity corresponds to a beam density $\approx 2.6 \times 10^{11} \text{ cm}^{-3}$, about 700 times the upstream beam density before compression. In addition to enabling these experiments, neutralized beam compression and focusing may make possible new high-gain direct drive targets with low range ions for heavy ion fusion.

Joint HIFS-VNL and GSI WDM experiments performed at the HHT area of GSI - Electron-cooled beams ($2.5 \cdot 10^9$ 238U⁷³⁺ ions at 350 MeV/u) from the SIS 18 storage ring compressed to 110 ns (FWHM) and focused at the target down to 150 μm diameter at GSI have been used in joint experiments to commission recently developed diagnostic instruments, and test different beam-target configurations for EOS studies, particularly two phase EOS of porous metals. The effect of pore size on behavior of porous and solid-density gold and copper targets was studied using existing diagnostics, for example, by measuring the target temperature as a function of pore size and comparing with

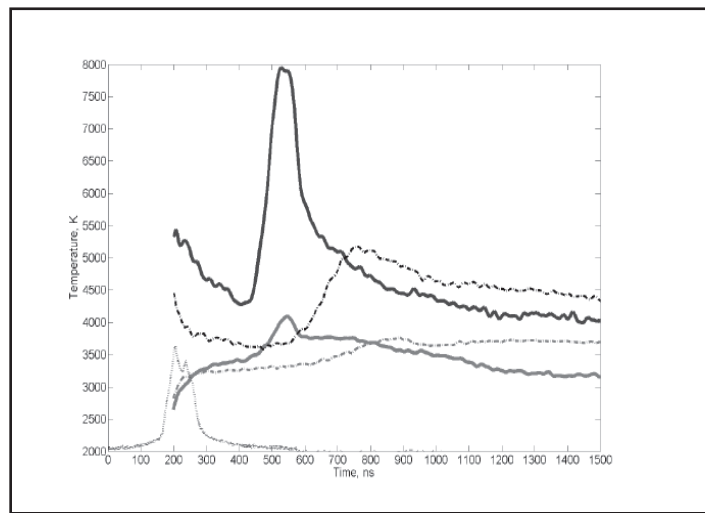


Figure 3: Figure 3: Pyrometer record comparing solid (solid lines) and porous (dashed lines) gold foils. Porous samples are 35% of solid density. Lower solid grey line- brightness temperatures at 900 nm, fitted, lower left: dotted line-temporal profile of heating beam in arbitrary units.

model predictions of the physics of porous targets (see Fig. 3). The analysis of experimental results and hydrodynamic simulations are in progress.

Progress in e-cloud research - Experiments were performed to study the matching and transport of a space-charge dominated ion beam in the solenoid transport channel of NDCX, including the effects of gas and electrons on the beam. The beam energy and current was the same as indicated above. Solenoid mid-planes are separated by 60 cm. Beam diagnostics are provided in an end tank. Long electrodes in the gaps were placed between magnets, and intercept magnetic flux that expands between magnets and passes through the

outer half of the beam radius in the center of solenoids. These “gap electrodes” are biased positively, in the clearing mode, to remove electrons. Short electrodes are provided in the center of each solenoid; these “solenoid electrodes” are biased negatively, in the clearing mode, to expel electrons from the solenoids. The biases can be reversed for a trapping mode: negatively-biased gap electrodes emit electrons due to ion or photon impact and repel trapped electrons, and positively-biased solenoid electrodes trap electrons in the center of each solenoid magnet. The trapping mode forms a Penning trap with magnetic radial confinement and electrostatic axial confinement of electrons. Images of the transverse beam structure taken about 5 μ s into a 10 μ s beam pulse with a 10-ns gate, show a clear difference between the clearing and trapping bias patterns (See Fig. 4). The coordinate space image for the clearing pattern shows a roughly circular 6.3-cm beam spot, with the density varying by about 25 % across the top plus a small 50% density depression at the center. The transverse phase space for this case shows a beam emittance of 20.9 mm-mrad and a convergence angle of -7.5 mrad. In contrast, a bias set to trap electrons has a larger spot size, a very irregular density profile, and an emittance that is five times larger than is found for the other bias pattern. The case with unbiased electrodes gave intermediate results, closer to the clearing than to the trapping case. Simulations of clearing and trapping cases provide reasonable agreement with the clearing case, but show little difference in the trapping case. This is possibly due to beam halo that scrapes the electrodes, producing electron and gas emission from the surfaces. Emission currents are measured from negatively biased electrodes consistent with this hypothesis. Without a mechanism to generate the observed gap-electrode current in the trapping case, simulations will not be able to reproduce the trapped electron density or its effects on the beam emittance. When electrons are minimized in either solenoids or magnetic quadrupoles, we find that the measured beam envelope agrees well with simulations. This suggests that we have a reasonable understanding of beam currents transport limits, in the absence of electron effects.

Integrated simulations - Two-dimensional (r,z) simulations were carried out using the LSP code to explore the limits to the current density achievable at the simultaneous focal plane with the NDCX experiment . A 327.4 keV, 21.5 mA K⁺ beam with a 1.43 cm radius was initialized with a 0.3 eV transverse and longitudinal temperature (0.126 mm-mrad rms normalized emittance). The beam was injected into the NDCX chamber (3.8 cm radius) just upstream of the 3 cm-wide acceleration gap with an initial pulse length of 0.7 μ s. The induction bunching module (IBM) imposes approximately a 10% velocity tilt (defined as $\delta v_z/v_z$) to the beam, which then drifts 15 cm through a region containing the electrostatic trap and permanent magnetic dipole that serve to confine the plasma in the drift region. The plasma from the 85 cm-long ferroelectric source ($n_{\text{pdrift}} = 5 \times 10^{10}$ cm⁻³, $T_{\text{pdrift}} = 3$ eV) was modeled between the magnetic dipole and a gate valve gap. An 80.5 kG, 9 cm-long final-focus solenoid filled with plasma was modeled (with fringe-

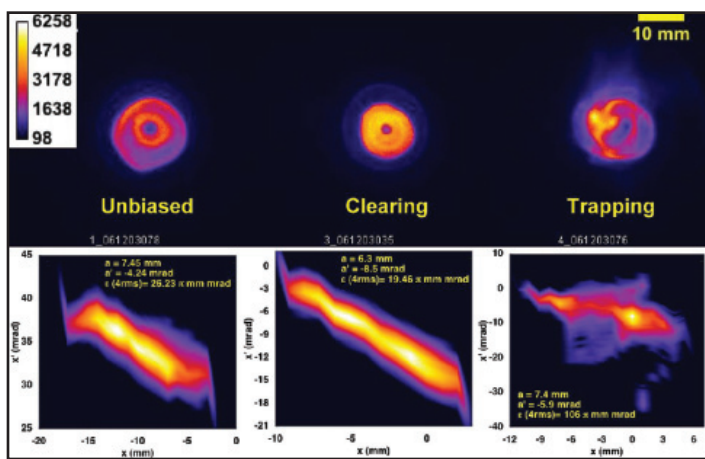


Figure 4: The simulation model includes the acceleration gap, electrostatic electron trap, permanent magnetic dipole, FEPS, clearance gap, final-focus solenoid, and FCAPS. (Bottom) Beam compression simulation results. The peak beam density (left) reached $4 \times 10^{12} \text{ cm}^{-3}$, the longitudinal current compression ratio was approximately 55X (middle), and the simultaneous radial spot size (1/e) was 0.47 mm (0.9 mm FWHM) with a peak on-axis cumulative energy deposition of 0.15 J cm^{-2} (right). The middle and right plots are color coded to show degree of pre-heat (200 ns total) on the target expected in this configuration.

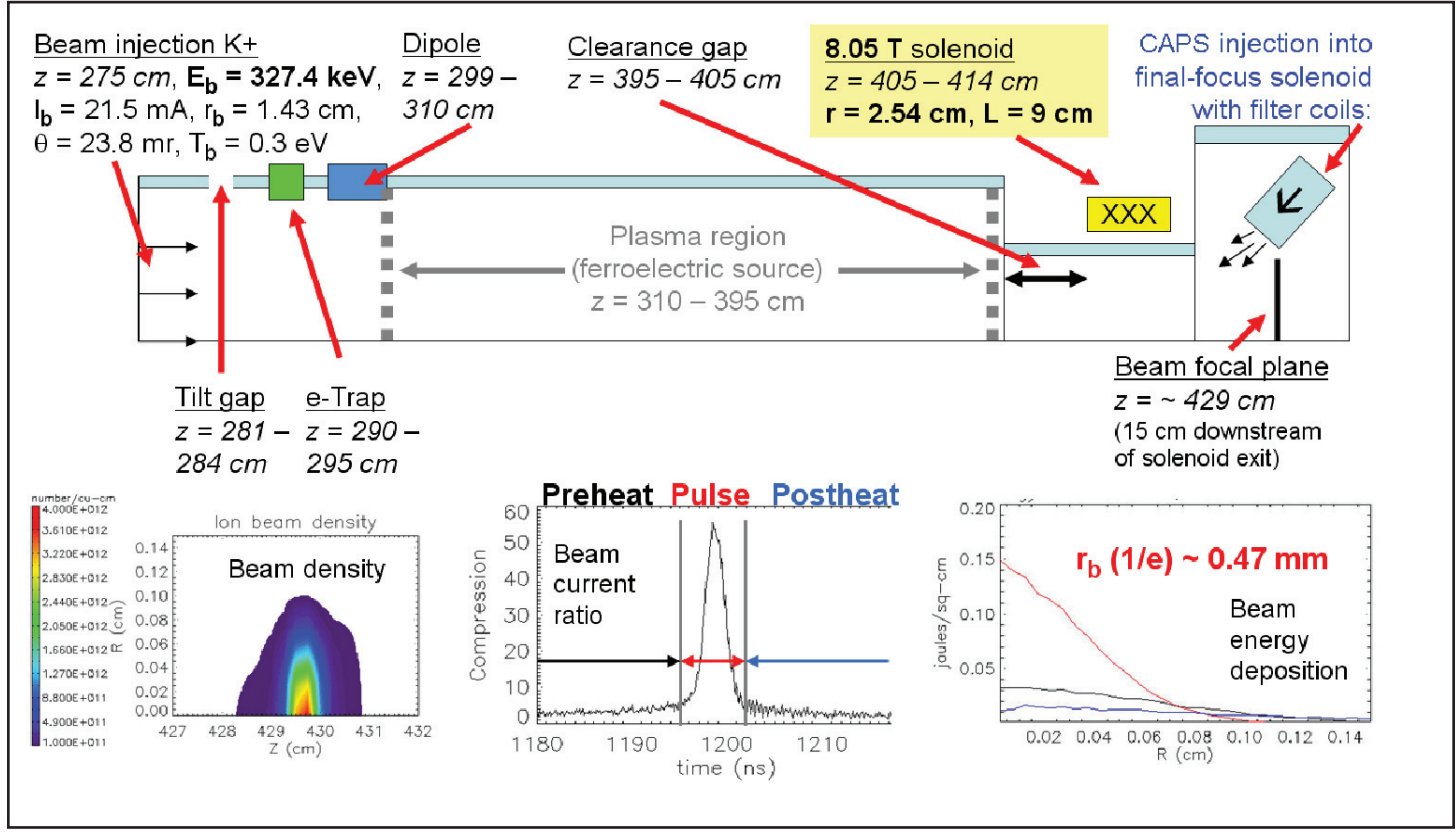


Figure 5: The simulation model includes the acceleration gap, electrostatic electron trap, permanent magnetic dipole, FEPS, clearance gap, final-focus solenoid, and FCAPS. (Bottom) Beam compression simulation results. The peak beam density (left) reached $4 \times 10^{12} \text{ cm}^{-3}$, the longitudinal current compression ratio was approximately 55X (middle), and the simultaneous radial spot size ($1/e$) was 0.47 mm (0.9 mm FWHM) with a peak on-axis cumulative energy deposition of 0.15 J cm^{-2} (right). The middle and right plots are color coded to show degree of pre-heat (200 ns total) on the target expected in this configuration.

fields) near the end of the drift region in order to ensure that the ion beam undergoes transverse focusing to a minimum spot size coincident with the longitudinal focal plane at $z = 429 \text{ cm}$, about 15 cm downstream of the exit of the final-focus solenoid. In this simulation, plasma is assumed to be everywhere to show the best possible focus, so actual experiments are expected to have larger focal spots; simulations involving realistic plasma flow profiles have predicted large focal spots by a factor of roughly two, indicating the need to increase the neutralizing plasma density in future experiments, especially near the target.

B.G. Logan, on behalf of the HIFSVNL